Stratospheric Effects of ENSO-Related Tropospheric Circulation Anomalies

MARK P. BALDWIN AND DONAL O'SULLIVAN

Northwest Research Associates, Inc., Bellevue, Washington

(Manuscript received 3 November 1992, in final form 9 January 1994)

ABSTRACT

Using 30 years of Northern Hemisphere geopotential data, from 1000 to 10 hPa, the link between three fundamental modes of tropospheric variability [the Pacific/North America (PNA), Western Pacific Oscillation (WPO), and Tropical/Northern Hemisphere (TNH) patterns] and the extratropical wintertime northern stratospheric circulation is explored. These modes of variability are known to be influenced by El Niño/Southern Oscillation (ENSO) and may provide a mechanism for ENSO to influence interannual variability of the stratospheric flow. Aside from any link to ENSO, these modes may be important in providing tropospheric wave forcing to the stratosphere.

These modes may be characterized by three of the leading rotated empirical orthogonal functions of the wintertime 500-hPa height field. An index of the amplitude of each of the modes is given by time series of principal components of that mode. By examining composites of years with high-index values minus years with low-index values it is shown that the zonal-mean stratospheric wind is not significantly influenced by any of the three tropospheric modes. However, the variability of these tropospheric modes appears to be associated with variations of stratospheric amplitudes of geopotential waves 1 and 2.

A comparison is made between the stratospheric influence of the equatorial quasi-biennial oscillation (QBO) and the three tropospheric modes during the December–February period. The influence from the QBO is weak in the troposphere and strongest in the stratosphere. The tropospheric modes' influence is strongest in the troposphere. At 50 hPa, the QBO's influence is a strong modulation of the strength of the polar night jet and, in terms of geopotential height, is about twice that of the PNA, WPO, or TNH modes. The effect of the QBO on the stratospheric climate appears to be considerably larger than that from the three tropospheric modes.

1. Introduction

It is now fairly well established that the equatorial quasi-biennial oscillation (QBO) acts to modulate the northern winter stratospheric circulation. This concept was first explored by Holton and Tan (1980, 1982), who showed that the 50-hPa polar vortex was considerably stronger during the west phase of the (50 hPa) equatorial QBO. Recently, Dunkerton and Baldwin (1991) and Baldwin and Dunkerton (1991) expanded on Holton and Tan's study to include more recent data and explore the mechanism by which planetary-scale wave propagation is modulated.

The QBO is one of several possible "external" influences on the interannual variability of the northern winter stratospheric flow. Other possible forcings include the solar cycle (with effects probably strongest in the equatorial upper stratosphere—associated with ozone heating), the remote effects of El Niño/Southern Oscillation (ENSO), and forcing from below by tropospheric circulation anomalies. Our approach in this paper is to examine the stratospheric circulation anomalies associated with those tropospheric modes that are linked to ENSO. This approach emphasizes the relationship between tropospheric circulation modes and changes to the stratospheric flow. The link from ENSO to stratospheric circulation anomalies is thus indirect.

One approach used to investigate ENSO's effect on the stratosphere is to compare directly some measure of ENSO with stratospheric variables. Wallace and Chang (1982) compared measures of the QBO and ENSO with the state of the polar vortex at 30 hPa. Van Loon and Labitzke (1987) examined the contributions to stratospheric interannual variability from ENSO. Both Wallace and Chang (1982) and van Loon and Labitzke (1987) showed that the phases of the QBO and ENSO tended to coincide, so that separation of the effects of ENSO from those of the QBO is difficult. Van Loon and Labitzke categorized each winter as cold, warm, or mean. During warm events, the polar vortex was found to be anomalously weak with an intense Aleutian high, while cold events were associated with a strong polar vortex and weak Aleutian high. To assess the effect of the QBO, they used only the mean years and found results similar to those of Holton and Tan.

Recently, Hamilton (1993a) performed calculations similar to van Loon and Labitzke's using data through

Corresponding author address: Dr. Mark P. Baldwin, Northwest Research Associates, Inc., P. O. Box 3027, Bellevue, WA 98009. E-mail: mark@nwra.com

1992. His investigation confirmed van Loon and Labitzke's earlier results. Hamilton also found that the composite differences in geopotential, using several different strategies to isolate ENSO effects from those of the QBO, were not statistically significant. Using the Geophysical Fluid Dynamics Laboratory "SKYHI" general circulation model (Fels et al. 1980), Hamilton (1993b) compared control model runs with model runs incorporating an enhanced region of sea surface temperature similar to that observed during warm ENSO events. The resulting stratospheric anomaly was quite similar to that observed. These results indicate that ENSO's stratospheric influence is probably genuine, but less than that of the QBO, and consists primarily of variations in wave amplitudes with a small effect on the zonal mean.

A fundamental difficulty in determining ENSO's stratospheric effects is to separate such associations from those of the QBO. If ENSO were uncorrelated with the QBO, and ENSO phases did not tend to match phases of the QBO, the problem would be minimized. By some measures of ENSO, the phases greatly overlap in the period since 1964, so that warm ENSO events are observed to coincide with an easterly QBO phase. If warm and cold ENSO events are defined as in van Loon and Labitzke (1987) and Hamilton (1993a) for the period 1964–1992, six of eight warm ENSO events occurred during easterly QBO years. Similarly, six of seven cold ENSO events happened when the QBO was westerly. In contrast, the correlation coefficient between the Tahiti–Darwin sea level pressure index [Southern Oscillation index or (SOI)] and Singapore 40-hPa wind (representative of the QBO) for 1964–1993 is only 0.03. In any case, it is desirable to separate the effects of the QBO from those of ENSO.

The question naturally arises as to whether or not the QBO and ENSO are somehow dynamically linked, resulting in the observed overlap of phases. The possible relationship between the QBO and ENSO has been investigated by several authors (Yasunari 1989; Geller and Zhang 1992; Gray et al. 1992; Angell 1992). An analysis of links between ENSO and QBO time series was made by Xu (1992), who found that the relationship between the two phenomena is not statistically significant. At this time, we know of no definitive evidence that the two phenomena are linked, although the possibility cannot be ruled out.

A further difficulty in separating the effects of ENSO and the QBO on the zonal-mean stratospheric circulation is that the stratosphere appears to have only one response to external forcing. In their empirical orthogonal function (EOF) analysis, Dunkerton and Baldwin (1992) showed that the leading spatial mode of zonally averaged zonal wind, having a dipole structure nearly identical to that of the response to the QBO, explained approximately 70% of the variance of December–January–February (DJF) means, even though the time series of this mode contained other signals besides the equatorial QBO. In the absence of wave driving, the polar vortex would be cold, strong, and undisturbed—similar to the Southern Hemispheric vortex. The zonal mean response to modulation of planetary-wave driving may not depend on the source of that modulation, whether from the QBO, ENSO, or extratropical troposphere.

Rather than examining a direct connection between ENSO and the extratropical stratosphere, we will consider that ENSO's effect on the stratosphere may be through modulation of the tropospheric flow. That is, ENSO may predispose the extratropical flow to a particular pattern(s) of low-frequency variability, which may then affect the stratosphere through vertical coupling. Three of the fundamental modes of variability of the midtropospheric flow [the Pacific/North America (PNA) mode (Wallace and Gutzler 1981), the Western Pacific Oscillation (WPO) (Wallace and Gutzler 1981), and the Tropical/Northern Hemisphere mode (TNH) (Livezey and Mo 1987; Barnston and Livezey 1987)] are observed to be linked to the state of ENSO. These modes may be seen with gridpoint correlations (e.g., Wallace and Gutzler 1981) or as leading rotated EOFs (e.g., Mo and Livezey 1986) of the midtropospheric extratropical flow. These modes of variability could act to communicate an ENSO signal to the stratosphere.

The degree to which ENSO can be said to influence each of these modes depends on the definition of a time series representative of ENSO and also on the time series of the amplitudes of the extratropical modes. Unfortunately, there is no single index that can characterize the state of ENSO. Various indices may be used as measures of the state of ENSO, including those based on SST, sea level pressure differences, 200- or 850-hPa wind anomalies, outgoing longwave radiation, and rainfall. If the SOI is used to define ENSO, then the sum of the variance associated with the three extratropical modes is 54%. The results are similar if the modes are defined by gridpoint anomalies. The correlations between the SOI and the EOF-based PNA, WPO, and TNH modes are −0.29, −0.27, and −0.62, respectively. Based on time series of gridpoint anomalies, which are not orthogonal, the correlations are −0.45, −0.35, and −0.53, respectively. Thus, most of the variance of each tropospheric mode is not associated with ENSO. We take the view that, for this analysis, the association of a precise fraction of ENSO variance with each tropospheric mode is not important. We assume that ENSO has some influence on the three tropospheric modes but does not explicitly refer to any ENSO index. Rather, we examine the relationships between the tropospheric modes of variability and the stratospheric flow.

As a measure of the amplitudes of the PNA, WPO, and TNH patterns, we use the time series of the principal component of the leading EOFs (using varimax rotation of 10 modes) that correspond closely to these

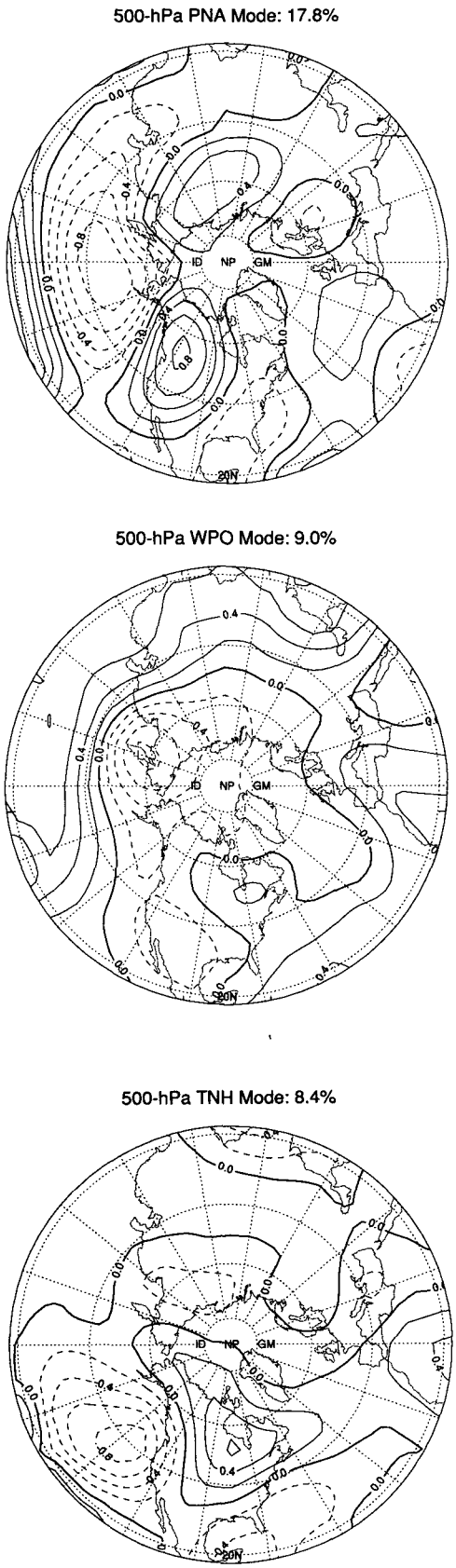

FIG. 1. Three of the leading rotated EOFs of the temporal covariance matrix of 500-hPa geopotential based on winter (December–February) for the years 1964–1993. Ten modes were rotated using varimax rotation. The value at each grid point is the correlation coefficient between the principal component time series and the geopotential anomalies at that point. The fraction of the variance over the domain explained by each mode is shown above each panel.

patterns. In this paper, these EOFs will be referred to as the "PNA-like mode," "the WPO-like mode," and the "TNH-like mode." Varimax rotation tends to localize the patterns and produces patterns that are closer to gridpoint-based correlations (e.g., Wallace and Gutzler 1981) than unrotated EOFs. The EOF-based definitions are used because they can be expected to be more stable than an index constructed from two, three, or four grid points. Most of the calculations were repeated using indices based on the gridpoint centers of action of the patterns. These results are considered in section 8.

The EOF-based time series of the extratropical modes are, fortuitously, nearly uncorrelated with the QBO. The correlation coefficients between the 40-hPa Singapore wind and the time series representing the PNA, WPO, and TNH modes are 0.14, −0.01, and 0.01, respectively. An alternate view is to compare the sign of the QBO with the sign of the three EOF-based time series. The QBO phase and the sign of the PNA and WPO time series are the same during exactly 50% of the years. Only the time series representing the TNH pattern shows some overlap. During 12 years, the TNH time series and the QBO have the same sign, and 18 years have the opposite sign.

2. Dataset, processing, and conventions

The data consist of National Meteorological Center 1200 UTC heights and temperatures daily for the period 1 January 1964 through 8 May 1993. These data are available north of 18°N at the levels 1000, 850, 700, 500, 400, 300, 250, 200, 150, 100, 70, 50, 30, and 10 hPa. Zonal-mean winds were calculated using the gradient balance method. The linear balance method (Hitchman et al. 1987; Robinson 1988) was used to calculate zonally asymmetric winds, which were needed for the Eliassen–Palm flux computations.

Seasonal-mean fields (both zonal-mean and horizontal grids) were then created for each DJF period from the daily data. These seasonal-mean fields were used in all of the calculations below. Correlations and composites involving grids of geopotential height were performed on a 4° latitude by 5° longitude grid.

EOFs were calculated from 30 DJF means of 500-hPa geopotential using the covariance matrix. The leading modes were then obtained using varimax rotation (Richman 1986). These modes were calculated using a 317-point polar stereographic grid that corre-

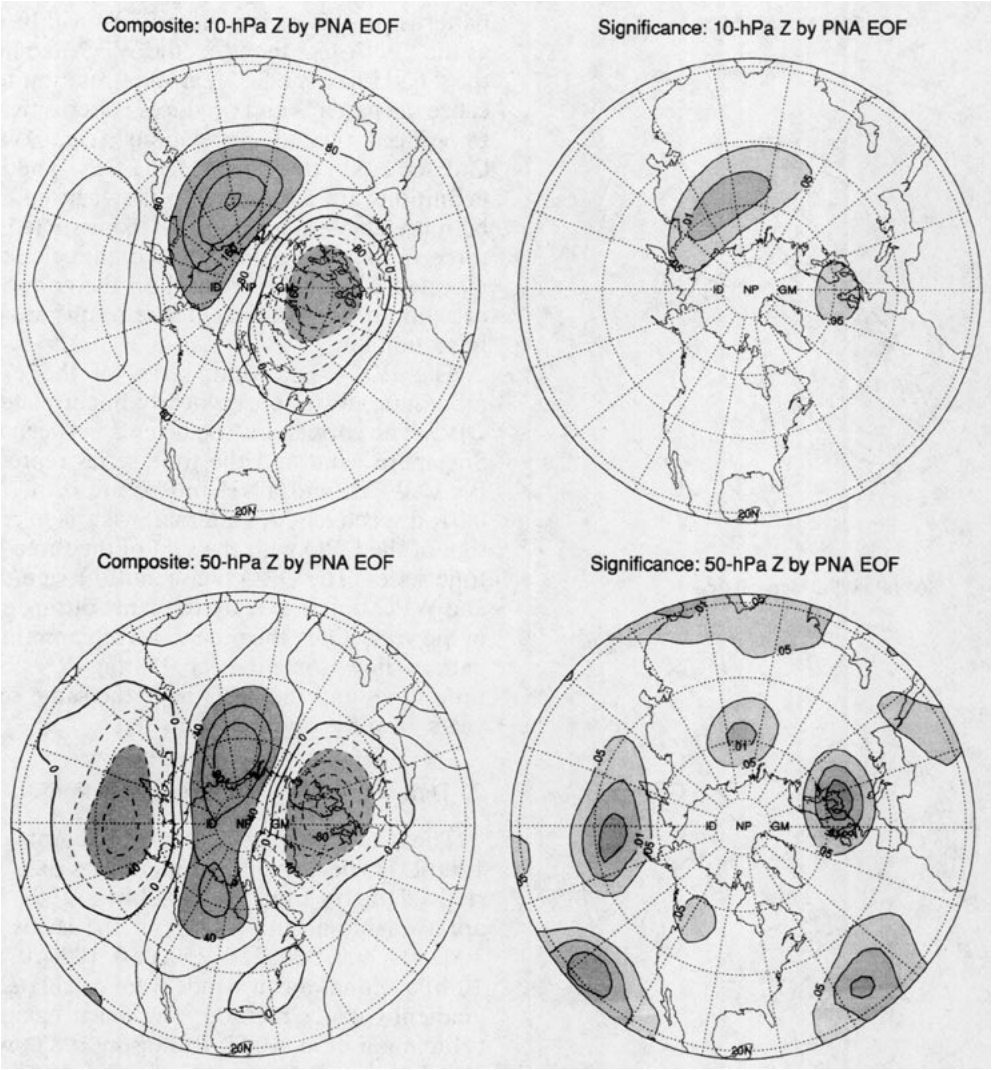

FIG. 2. Geopotential composites created by averaging all years in which the time series of the expansion coefficients of the PNA-like EOF was positive and subtracting all years in which it was negative. Panels on the left side of the figure show composite differences (m). The contour interval is 20 m for 500–50 hPa and 40 m at 10 hPa. Absolute values greater than 40 m are shaded for 500–50 hPa and greater than 120 m at 10 hPa. Panels on the right side show corresponding significance levels based on a one-sided t test. Values significant at more than the 0.05 level are shaded. The levels contoured are 0.05, 0.01, 0.003, 0.001, 0.0003, 0.0001, 0.00003, . . .

sponds to approximately 6° latitude horizontal resolution. The time series of the amplitudes of the modes (principal components) of the PNA-, WPO-, and TNH-like modes are orthogonal and used as indices of the amplitudes of the respective patterns. The resulting principal component time series were not sensitive to the number of leading EOFs used in the varimax procedure. Ten modes are used for all computations presented below, although the results are very similar if 8–12 modes are rotated.

The signs of the EOF patterns calculated by this method are arbitrary. To be consistent with recent literature, the signs of the indices were adjusted so that, at 500 hPa, the PNA pattern has positive values over western North America. The WPO pattern is negative in the northern part of its dipole, while the TNH pattern has a positive center over eastern North America (Fig. 1).

The QBO time series data consist of the DJF average of the 40-hPa (the average of 30 and 50 hPa) Singapore (1°N) wind. The tropical stratospheric zonal wind is nearly zonally symmetric, so any individual station near the equator is fairly representative of the zonal mean.

3. Statistical analysis

The composite difference maps shown below are either horizontal hemispheric maps of geopotential or

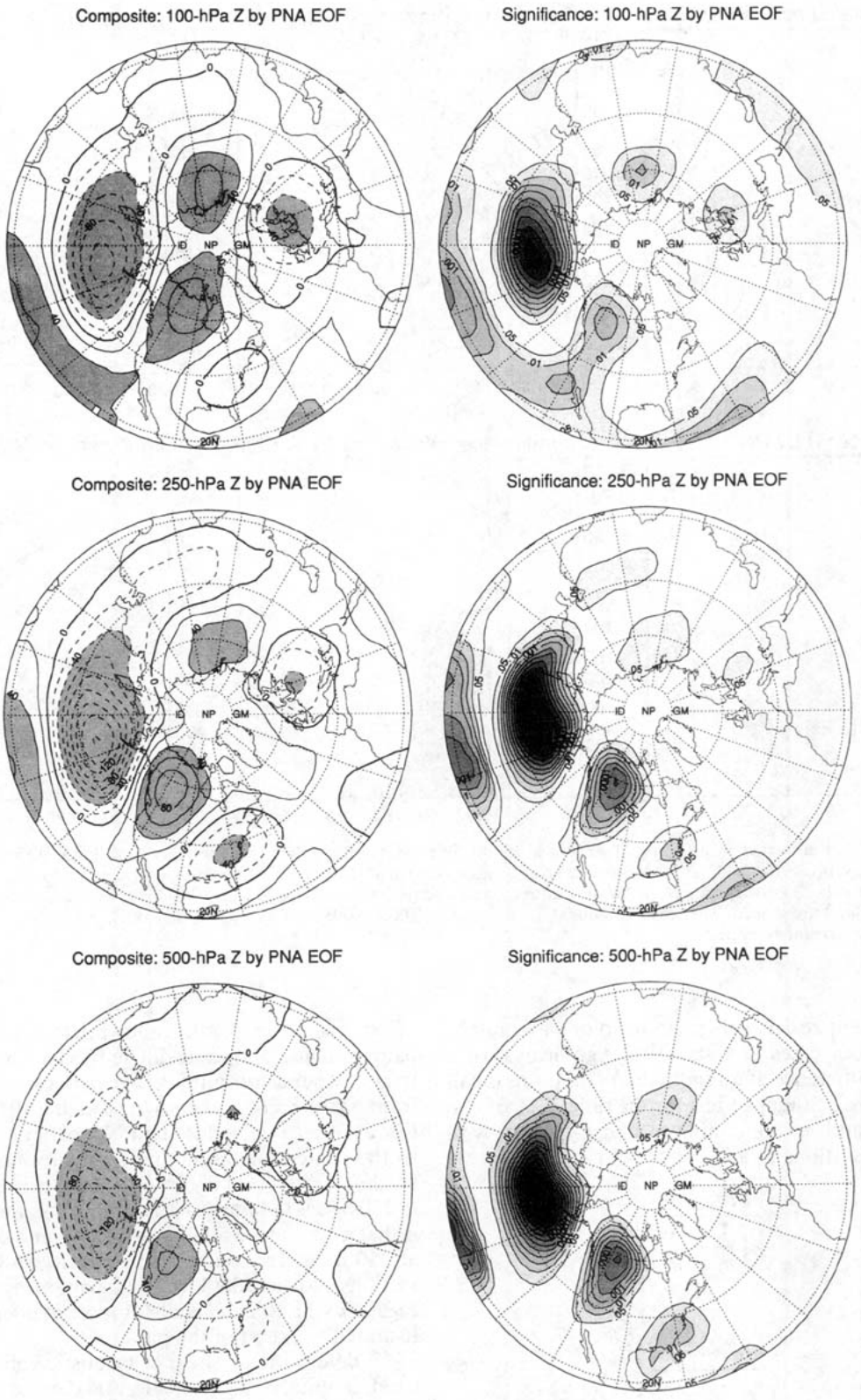

FIG. 2. (*Continued*)

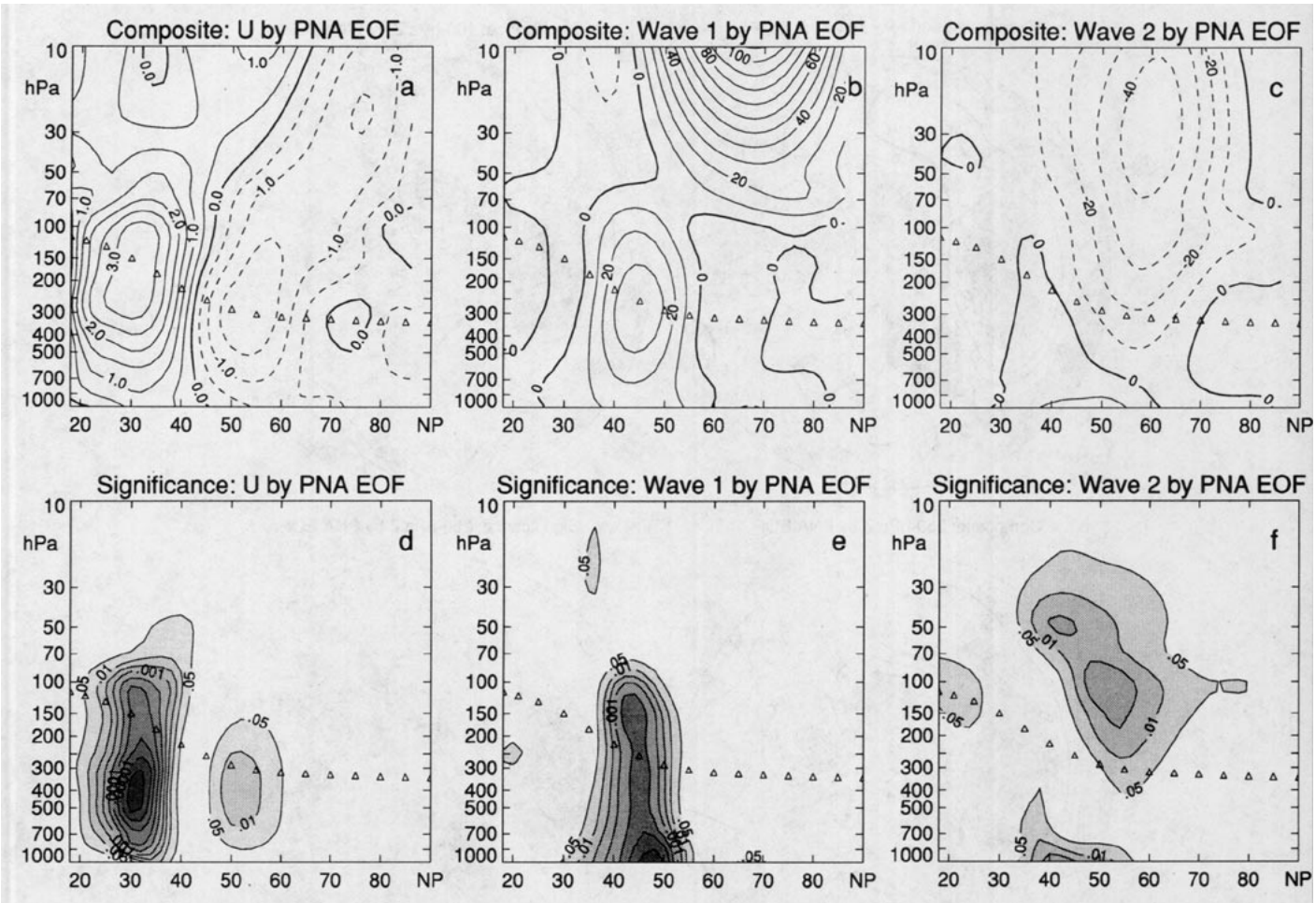

FIG. 3. Composites created by averaging all years in which the time series of the expansion coefficients of the PNA-like EOF was positive and subtracting all years in which it was negative: (a) zonal-mean wind (m s^{-1}); (b) amplitude of zonal wavenumber 1 (m); (c) amplitude of zonal wavenumber 2 (m). The panels below show corresponding significance levels based on a one-sided t test. Values significant at more than the 0.05 level are shaded. The levels contoured are 0.05, 0.01, 0.003, 0.001, 0.0003, 0.0001, 0.00003, ... Triangles represent the approximate wintertime tropopause.

latitude–height zonal averages of wind or wave amplitudes. In both cases, the statistical significance of a composite difference at an individual grid point is calculated using a Student t-test for the difference of two means, m_1 and m_2 containing n_1 and n_2 points, with standard deviations σ_1 and σ_2:

$$t = \frac{m_1 - m_2}{\sigma\left(\frac{1}{n_1} - \frac{1}{n_2}\right)^{1/2}} \tag{1}$$

and

$$\sigma = \left(\frac{n_1\sigma_1^2 + n_2\sigma_2^2}{n_1 + n_2 - 2}\right)^{1/2}. \tag{2}$$

From these values of the t statistic, a one-tailed t test is performed to estimate the significance of each composite difference. A one-tailed test, rather than a two-tailed test, is used for the following reasons: the spatial patterns in the composite differences tend to be spatially large scale and continuous. The patterns also originate from a pattern of known sign (e.g., the PNA pattern). For example, we define the PNA pattern at 500 hPa, so the centers of action and signs are known at that level. If a grid point above one of the centers of action at 250 hPa is to be tested for significance, the hypothesis is that a composite difference of the same sign is found at 250 hPa. Horizontal maps or latitude–height cross sections showing the local significance levels are used together with dimensional composite differences to illustrate the extent of the patterns.

To determine if a field of t statistic values is significant, a suitable test statistic was devised to estimate how likely such a field would be to occur by chance (Livezey and Chen 1983; Barnston and Livezey 1989). For the latitude–height cross sections, the value of t is averaged over the stratosphere (taken to be all grid

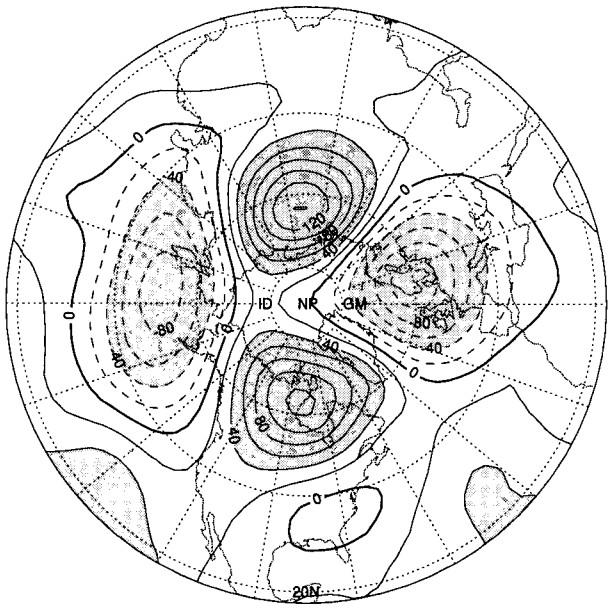

FIG. 4. The 50-hPa geopotential composites created by averaging all years in which the time series of the expansion coefficients of the PNA-like EOF was positive and subtracting the average of all years for which the time series was negative. The calculation includes only those years when the QBO was westerly. The contour interval for both panels is 20 m. Values greater than 40 m and less than −40 m and shaded.

points from 150 to 10 hPa). For the horizontal maps, t is first averaged over longitude and then over latitude, to be consistent with the method used for the cross sections.

To estimate the significance of the integrated t statistic, Monte Carlo simulations were performed in which the categorization of each year was randomly assigned, keeping the same number of years in each category (e.g., 15/15). For each data field, 10 000 simulations were performed with random assignments of each year to each composite category. For each simulation, the integrated t statistic was calculated. Thus, for each data field, a distribution of the integrated t statistic was obtained. The significance of an observed integrated t value is then estimated by comparison to this t statistic distribution.

It should be emphasized that the field significance calculations are only *estimates* and will be treated as general guides. For the latitude–height cross sections, the method described above equally weights grid points from 150 to 10 hPa and from 18°N to the pole. The region used, as well as any latitudinal weighting, is a subjective choice. The application of field significance to the horizontal maps is more problematic. The varimax rotation procedure produces EOFs that are regional structures, but the integrated t statistic tests the entire grid. For this reason the change with height of the field significance will be emphasized.

4. Stratospheric features associated with the PNA pattern

Figure 1a illustrates the PNA-like mode obtained by varimax rotation of the leading 10 EOFs. The value at each grid point is the correlation coefficient between the time series of the principal component of that mode and the geopotential anomalies at that point. The PNA-like mode accounts for 17.8% of the variance of the field.

The series of plots in Fig. 2 illustrates the vertical variation of the horizontal structure of the composite difference of geopotential between years with positive and negative values of the time series of the amplitude of the PNA EOF. Each panel in the left column was created by taking the difference between the average geopotential height during winters when the time series of the principal components was positive and subtracting the average when it was negative. The corresponding panels in the right-hand column show contours of the local significance level of the composite difference.

With increasing height, the PNA pattern becomes weaker but is recognizable at 100 hPa. The centers of action remain geographically fixed. At 500 hPa, the main features compose the PNA pattern with only a few outlying areas significant at the 0.05 level. The value of the integrated t statistic at 500 hPa is 1.27, with a value of 1.22 significant at the 0.05 level. Even at the level where the pattern is defined, the average value of the t statistic indicates significance at only the 0.05 level. This illustrates that because the PNA pattern is confined to one region, the hemispheric measure of its significance is only moderate. The integrated t sta-

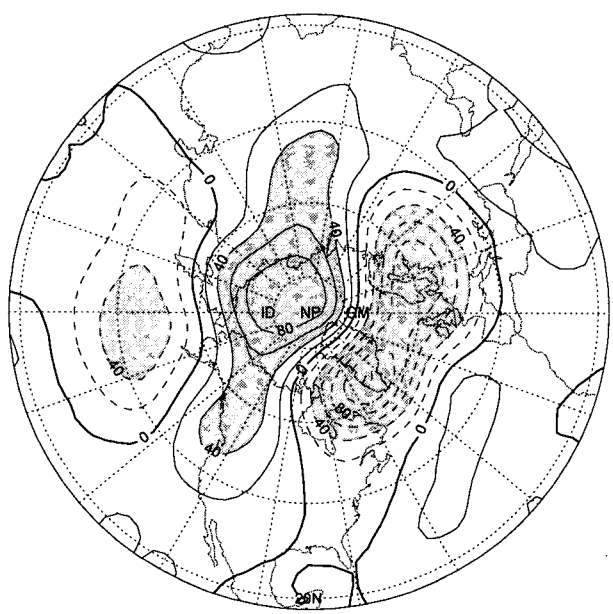

FIG. 5. As in Fig. 4 except only years in which the QBO was easterly were used.

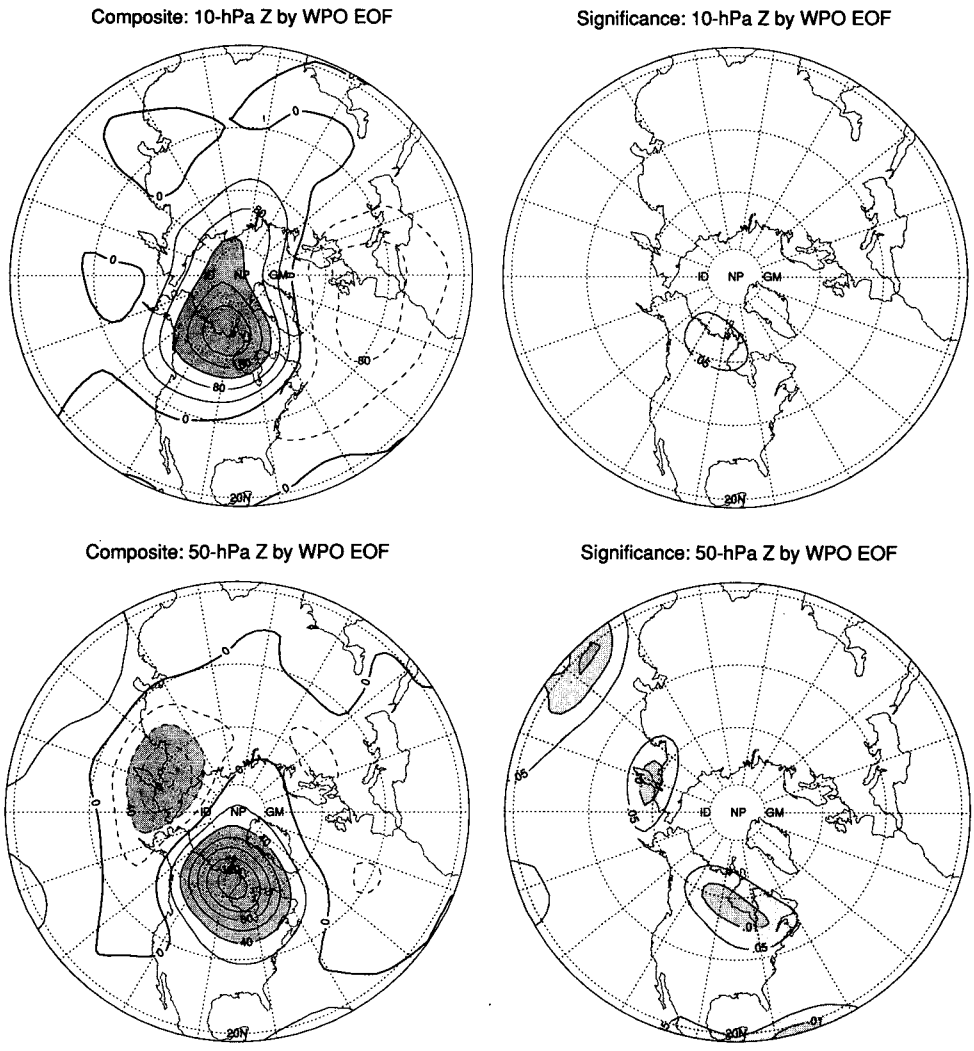

FIG. 6. As in Fig. 2 except the time series of the expansion coefficients of the WPO-like EOF was used to create the composites.

tistic indicates that the PNA anomalies remain significant at the 0.05 level up to 100 hPa but drops off substantially above that level.

At 250 hPa, another center near 90°E can be seen. This feature, together with a center near the Greenwich meridian (visible at 250 hPa and higher) form a wave-2 pattern that dominates the stratosphere. As the PNA pattern becomes weaker with height, anomalies near 90°E and the Greenwich meridian dominate the pattern (e.g., at 10 hPa). This filtering of higher wavenumbers in the stratosphere is consistent with the linear propagation ideas originating with Charney and Drazin (1961). The wave-2 pattern can be seen most clearly at the 50-hPa level. This figure corresponds to Holton and Tan's (1980) 50-hPa geopotential composites based on the sign of the QBO. Only at the 50- and 10-hPa levels is there even a small anomaly near the pole. This contrasts with composites based on the QBO (section 7), in which the polar vortex is strongly modulated.

The zonal-mean PNA signal is illustrated in Fig. 3, showing composite differences between years with positive and negative values of the time series of the amplitude of the PNA-like mode. Figure 3a illustrates the zonal wind composite difference that is dominated by a tropospheric dipole centered on about 40°N. This structure is mainly confined to below 70 hPa, with a small anomaly in the middle stratosphere (near the 10-hPa level). Figure 3d shows the corresponding values of local significance that decrease sharply above the tropopause. The large interannual variability of the polar night jet makes the stratospheric composite differences of about 1 m s^{-1} insignificant.

The zonal-mean anomaly in wave-1 amplitude is shown in Fig. 3b. Although there is a substantial modulation of wave-1 amplitude at about 40°N in the tro-

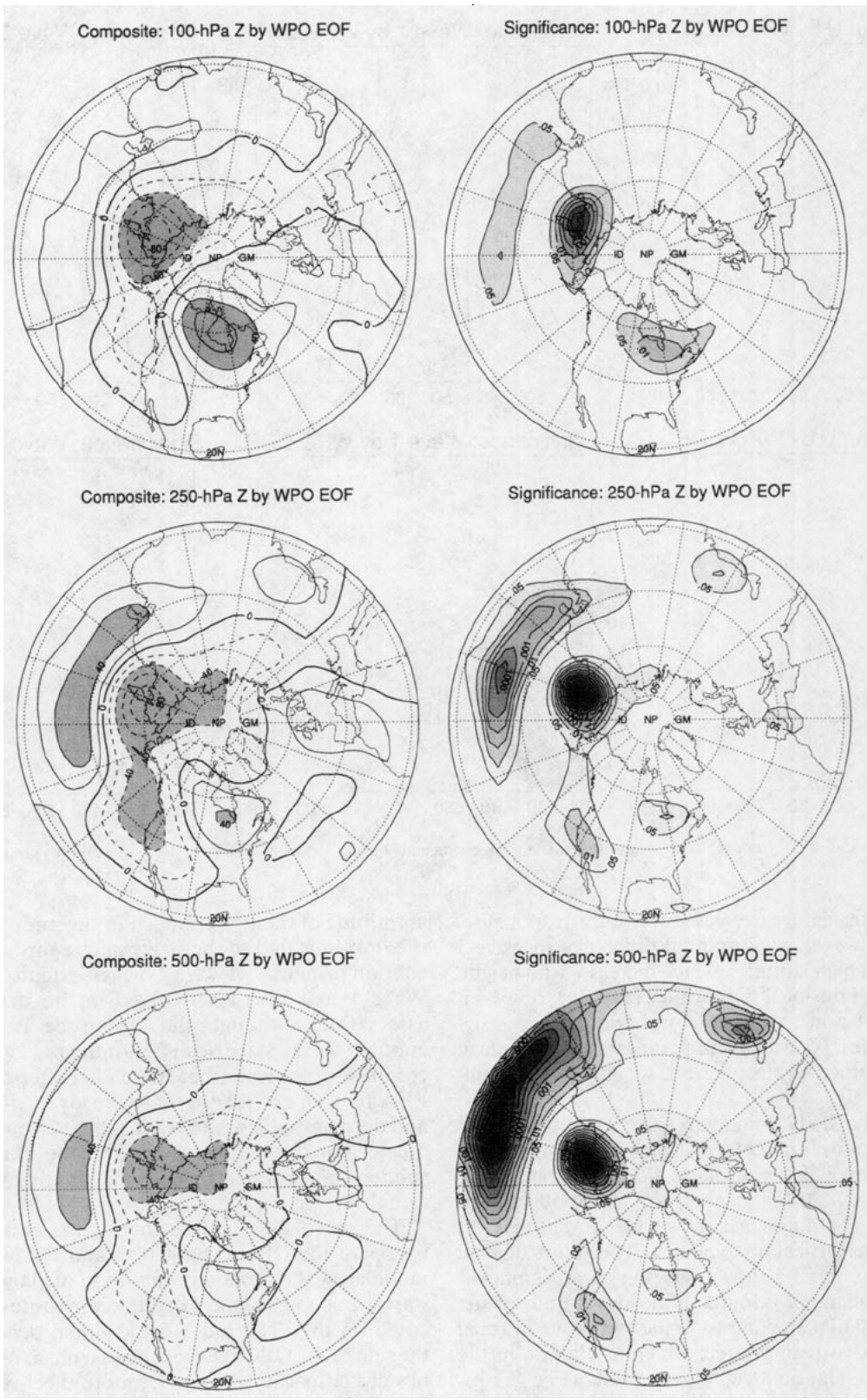

FIG. 6. (*Continued*)

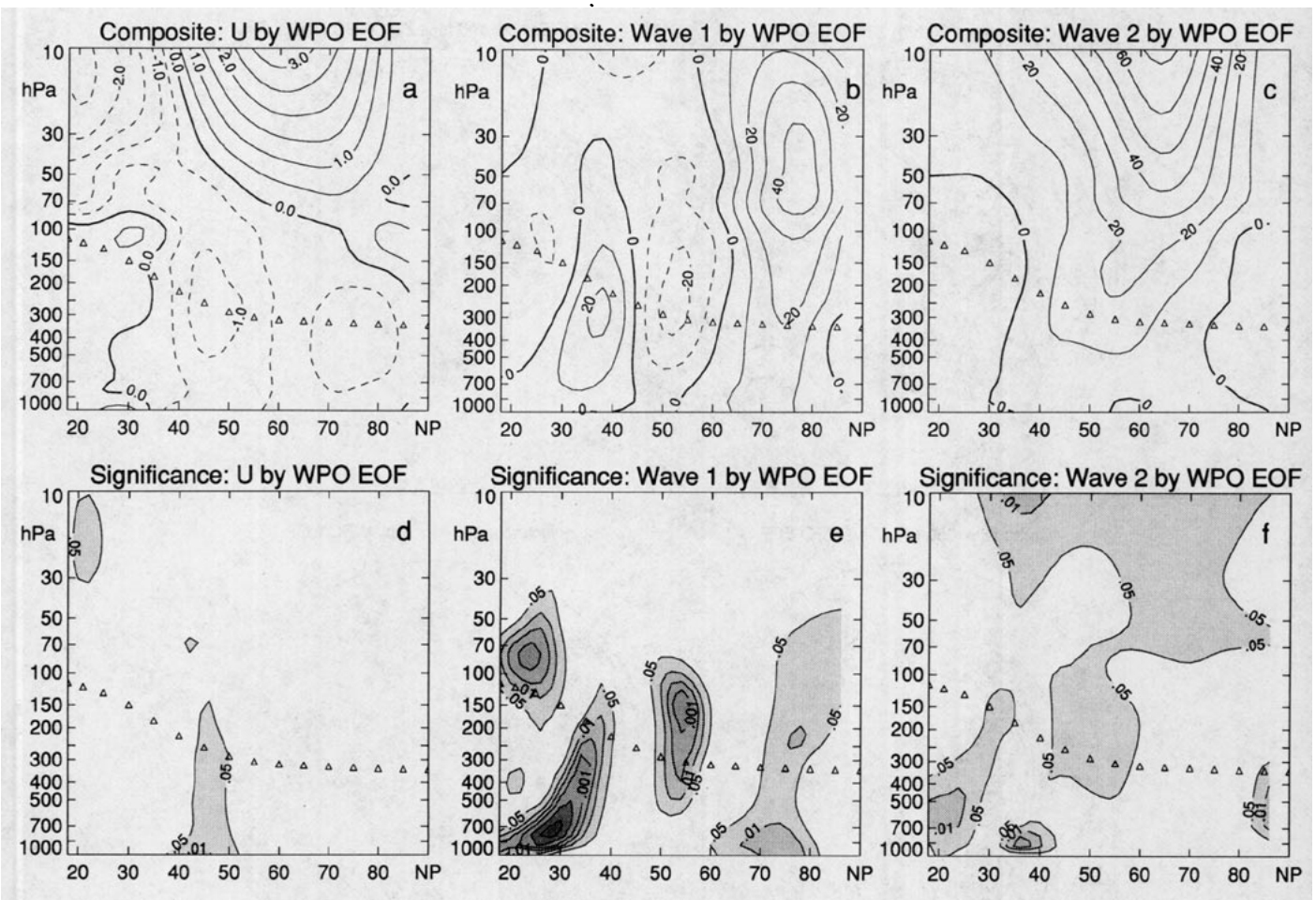

FIG. 7. As in Fig. 3 except the time series of the expansion coefficients of the WPO-like EOF was used to create the composites.

posphere, this feature decreases above the tropopause. There is, however, a substantial difference in wave-1 amplitude at high latitudes, which increases with height. The values of the local significance (Fig. 3e), however, indicate that none of the stratospheric pattern is significant at the 0.05 level. Field significance tests confirm that the average stratospheric association is not unusual.

The composited anomaly in wave 2 is illustrated as Fig. 3c. The amplitude of wave 2 increases with height above the tropopause and affects the entire stratosphere north of 40°N. Although the response at 500 hPa is very small, the difference in wave-2 amplitudes increases in the vertical up to 30 hPa. The values of local significance (Fig. 3f) shows that the most significant composite difference is found in the lower stratosphere, peaking at 50 hPa, in contrast to the composite in zonal wind and wave-1 amplitude, which are largest in the troposphere. The field significance tests (Fig. 3f) indicate that this association is significant at the 0.05 level.

Based on the horizontal correlation maps and the wave-2 composites, it appears that modulation of the amplitude of the PNA pattern in the midtroposphere is communicated to the stratosphere through the excitation primarily of wave 2, which extends vertically. Wave 1 may also be involved in the stratospheric association, although the amplitude is not large enough to be statistically significant. Zonal wind composites indicate that these characteristics of the PNA pattern extend only into the lower stratosphere and decay rapidly with height. These calculations indicate that the polar vortex, and the likelihood of sudden warmings, is not affected greatly by the PNA signal.

The mean flow is different for the east and west phases of the QBO (Dunkerton and Baldwin 1991), modulating the upward propagation of planetary-scale waves. One might expect that the composite differences based on the PNA index could differ, depending on the sign of the QBO. During the east phase of the QBO, upward propagating waves are more effective at changing the high-latitude zonal-mean flow. Figure 4 illustrates composites at 50 hPa for the west QBO phase, while Fig. 5 illustrates the east QBO phase. The pattern of wave 2 is evident in both composites. The east-phase

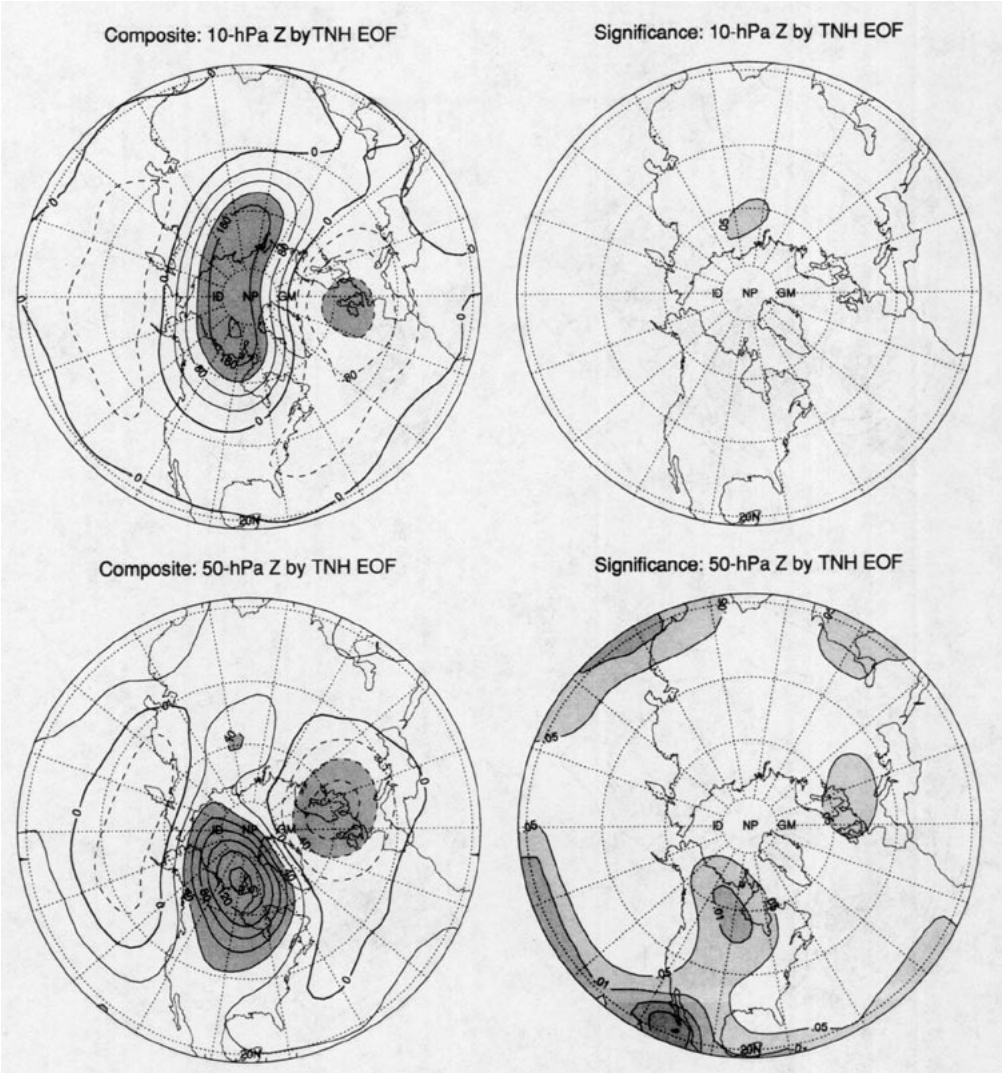

FIG. 8. As in Fig. 2 except the time series of the expansion coefficients of the TNH-like EOF was used to create the composites.

composite is more zonally symmetric with a larger composite difference over the polar cap. Although this result is consistent with the idea that the QBO affects the vertical propagation of tropospheric waves, the difference between these composites is not large and the composites are not statistically significant at the 0.05 level.

5. Stratospheric features associated with the WPO pattern

Figure 6 illustrates composite geopotential anomalies based on the time series of the principal component of the WPO-like EOF. The WPO pattern is clearly visible at 500 and 250 hPa. At 100 hPa, the North Pacific center is dominant, while a new center over Canada is visible. This pattern continues at 50 hPa, with only the Canadian center remaining at 10 hPa. Values of the integrated t statistic drop from 1.23 at 250 hPa (significant at the 0.05 level) to 0.76 at 100 hPa, well below the 1.27 needed for significance at the 0.05 level. One would expect the 500- and 250-hPa responses to be genuine. More important is the decrease with height, indicating that the response decreases above the tropopause.

Composites of zonal-mean values of wind, wave-1 amplitude, and wave-2 amplitude (Fig. 7) provide an additional view of the WPO association. The small difference in the composite of zonal wind (Fig. 7a) is significant at the 0.05 level only at small number of grid points (Fig. 7d). Similarly, the wave-1 composite difference is small (Figs. 7b,e). However, the wave-2 composite, shown in Figs. 7c, f, is field significant at the 0.05 level. The geopotential response (e.g., 50 hPa in Fig. 6) projects mostly onto wave 2. Although the wave-2 composite difference is nowhere large, about

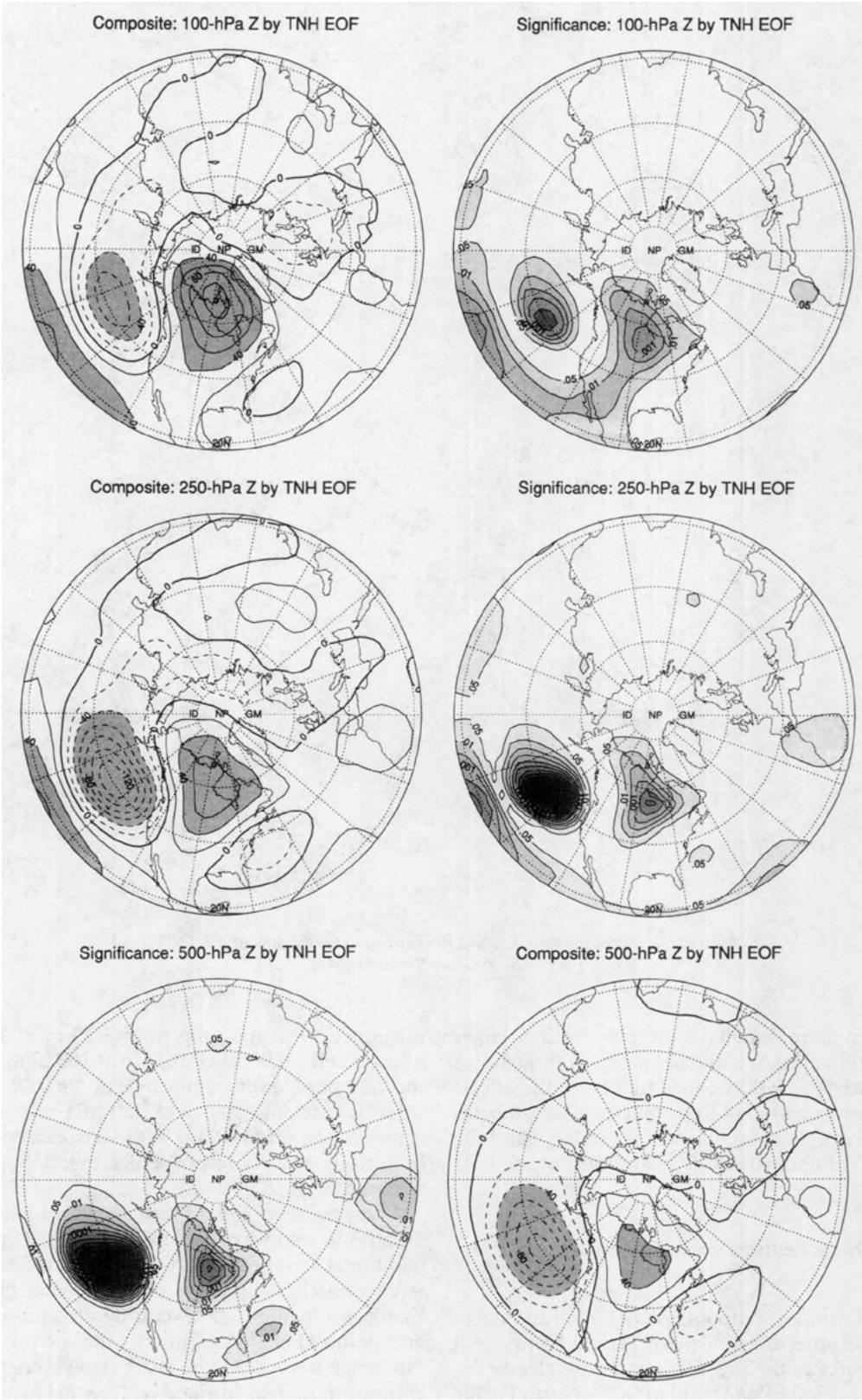

FIG. 8. (*Continued*)

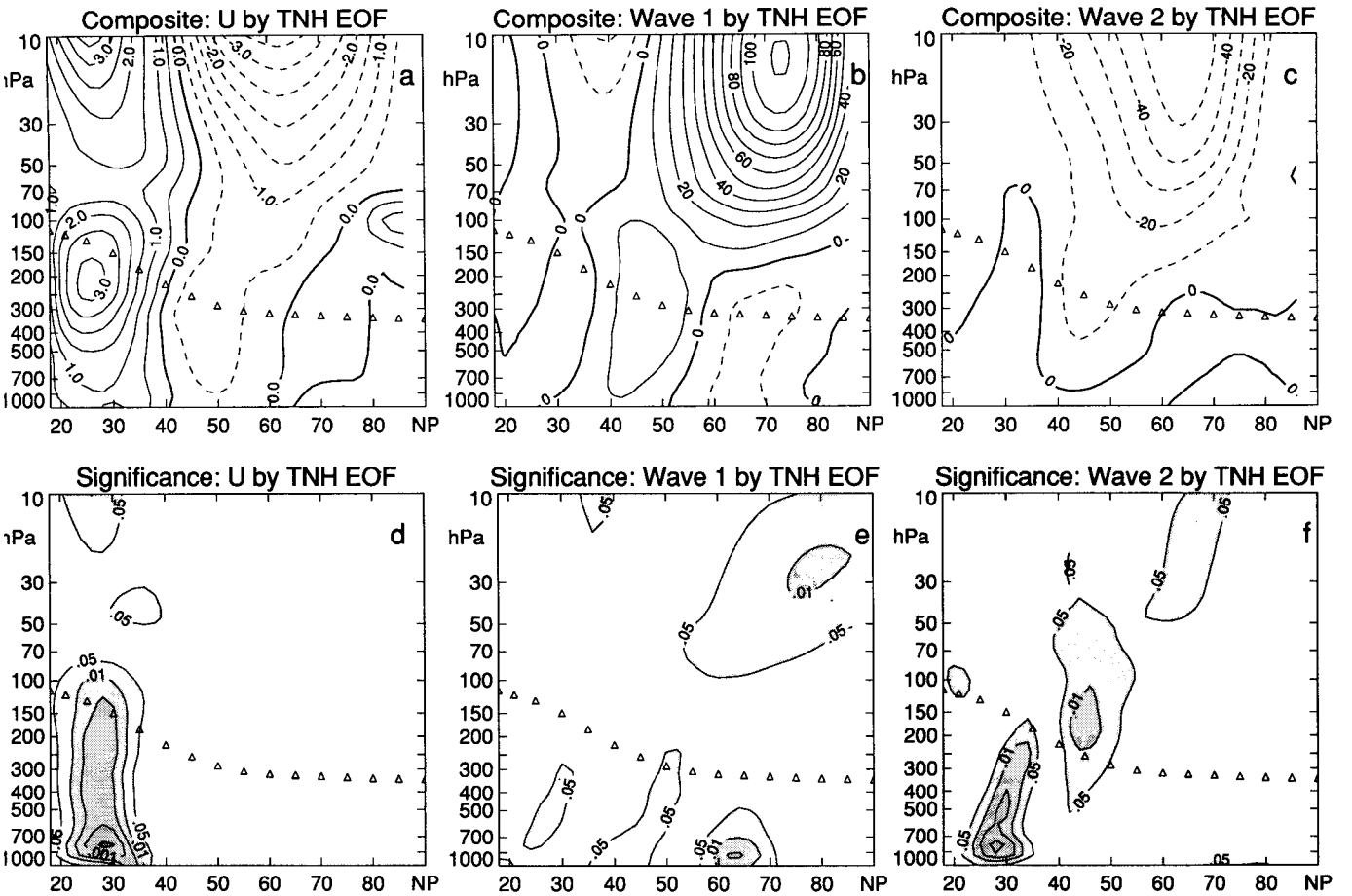

FIG. 9. As in Fig. 3 except the time series of the expansion coefficients of the TNH-like EOF was used to create the composites.

half the stratospheric grid exceeds the local 0.05 significance level.

Based on these composites, the stratospheric association to the WPO-like EOF appears to be weak but probably real. The effect on the zonal-mean flow is negligible, so an influence on the likelihood of sudden warmings is unlikely. The response appears to be confined to a high-latitude pattern with centers over Canada and the North Pacific, which projects primarily onto zonal wave 2.

6. Stratospheric features associated with the TNH pattern

The geopotential composites based on the time series of the principal component of the TNH-like EOF are shown in Fig. 8. The TNH pattern is clearly visible at tropospheric levels and at 100 hPa. At 50 hPa, only the Canadian center remains, with a smaller feature of opposite sign over Europe. At 10 hPa, the composite difference is weaker and centered near the pole. Unlike the WPO response, the 500-hPa TNH pattern is confined to a very small area of the grid. Consequently, the tropospheric-integrated t statistic values (0.98 at 500 hPa) are not significant at the 0.05 level (1.22 would be required). This again illustrates a shortcoming of the use of a hemispherically integrated quantity to measure the statistical significance of what is really a locally confined pattern. However, the values of the integrated t statistic remain near 1.0 through 50 hPa and drop to 0.67 only at 10 hPa.

The zonal-mean wind composite (Fig. 9a,d) is small and not significant in the stratosphere. The amplitudes of wave 1 and wave 2 (Figs. 9b,c,e, f) are moderate but not significant at the 0.05 level. Since the geopotential TNH composite differences are relatively small, the associated wave amplitudes cannot be expected to be large. Both wave 1 and wave 2 show locally significant values in the stratosphere poleward of 40°N. Like the WPO response, the tropospheric TNH pattern is associated with changes in stratospheric wave amplitudes and local geopotential anomalies but with very little change to the zonal-mean flow.

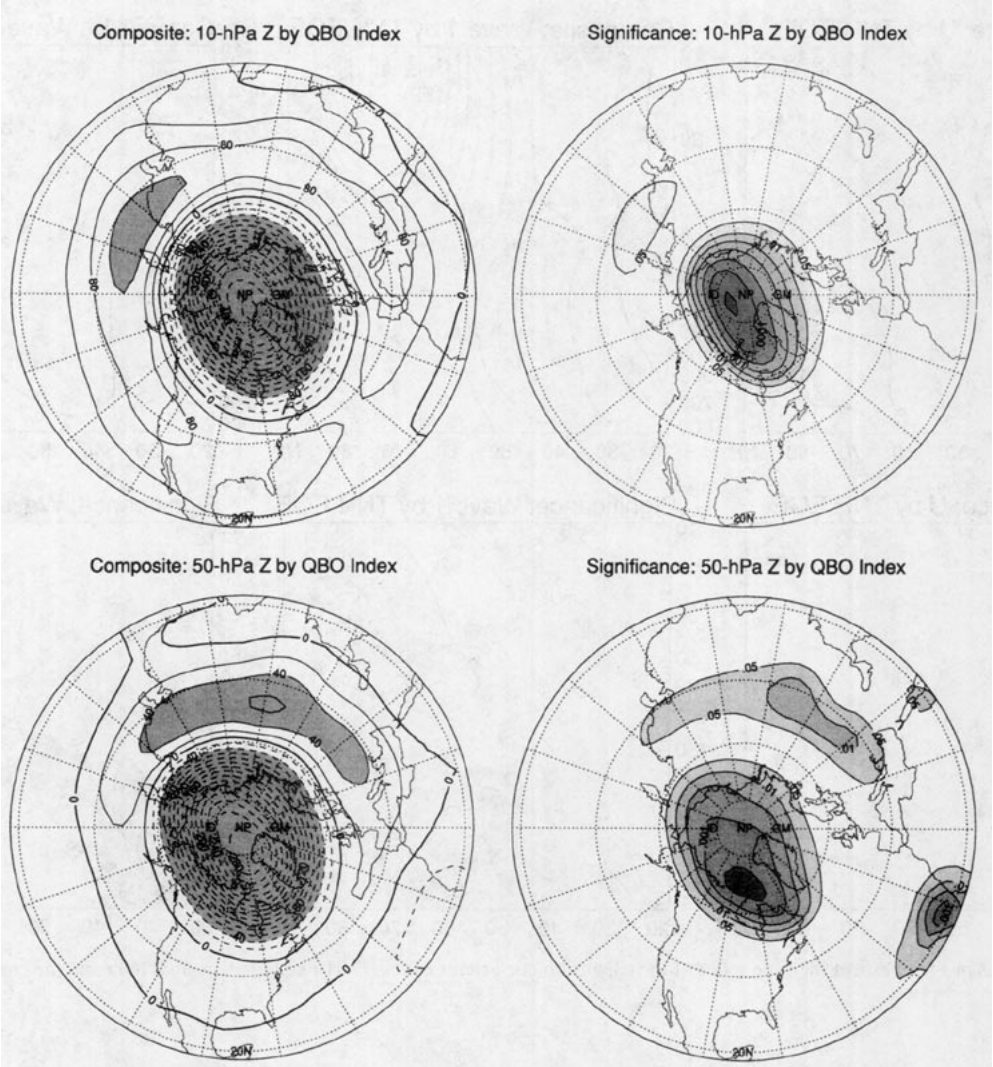

FIG. 10. As in Fig. 2 except the time series of the 40-hPa Singapore wind was used to create the composites.

7. Comparison with effects of the QBO

After examining the stratospheric response associated with tropospheric modes of variability, a comparison with the influence from the QBO is appropriate. The stratospheric response to the QBO is modulation of the zonal-mean wind. Composite differences were created using the time series of the DJF zonal wind at Singapore at 40 hPa in a manner similar to that used to create the PNA, WPO, and TNH composites. Figure 10 illustrates the composite differences in geopotential based on the QBO. The signature of the QBO is negligible at 500 hPa but becomes significant at the 0.05 level at 100 hPa. At 10 hPa, the value of the integrated t statistic indicates significance at the 0.001 level. The maximum composite difference in geopotential height at 50 hPa is slightly more than 280 m, about twice the amplitude at any individual grid point from the three tropospheric modes.

Figures 11a,d show the composite difference in zonal-mean wind. This response is characteristic of the first EOF of zonal-mean wind (Nigam 1990; Dunkerton and Baldwin 1992). The local significance values (Fig. 11d) increase upward through the middle stratosphere, in contrast to the patterns associated with the tropospheric EOFs that tend to decay above 100 hPa. The observed response is consistent with that from modeling studies in which the QBO was varied (O'Sullivan and Young 1992). Unlike the PNA and WPO responses, the effect of the QBO is primarily to modulate the strength of the polar vortex.

The amplitudes of waves 1 and 2 in the stratospheric composite differences (Figs. 11b,c,e, f) are moderate. Although not field significant at the 0.05 level, the stratospheric composite difference in wave-2 amplitude, which can be seen as an elon-

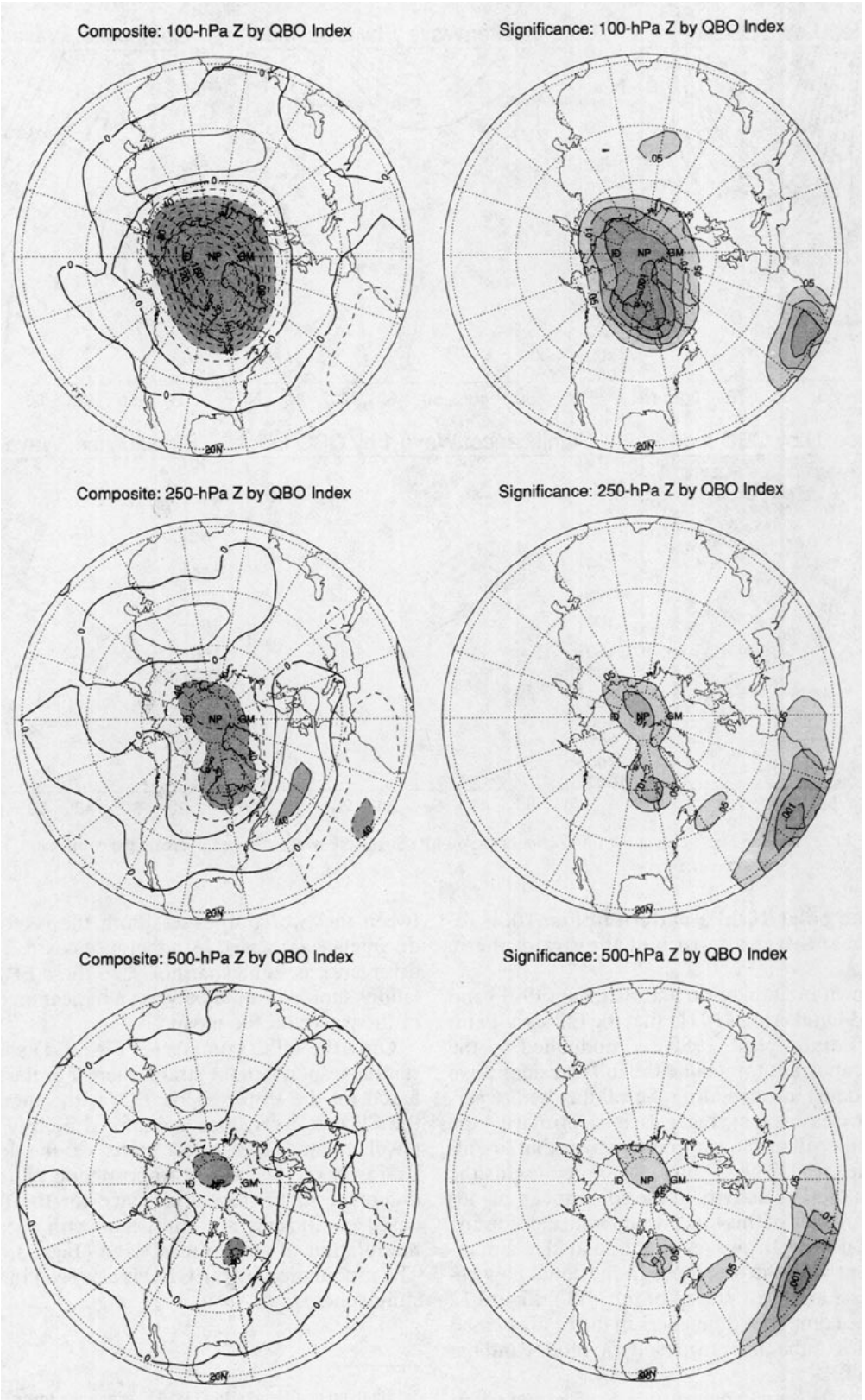

FIG. 10. (*Continued*)

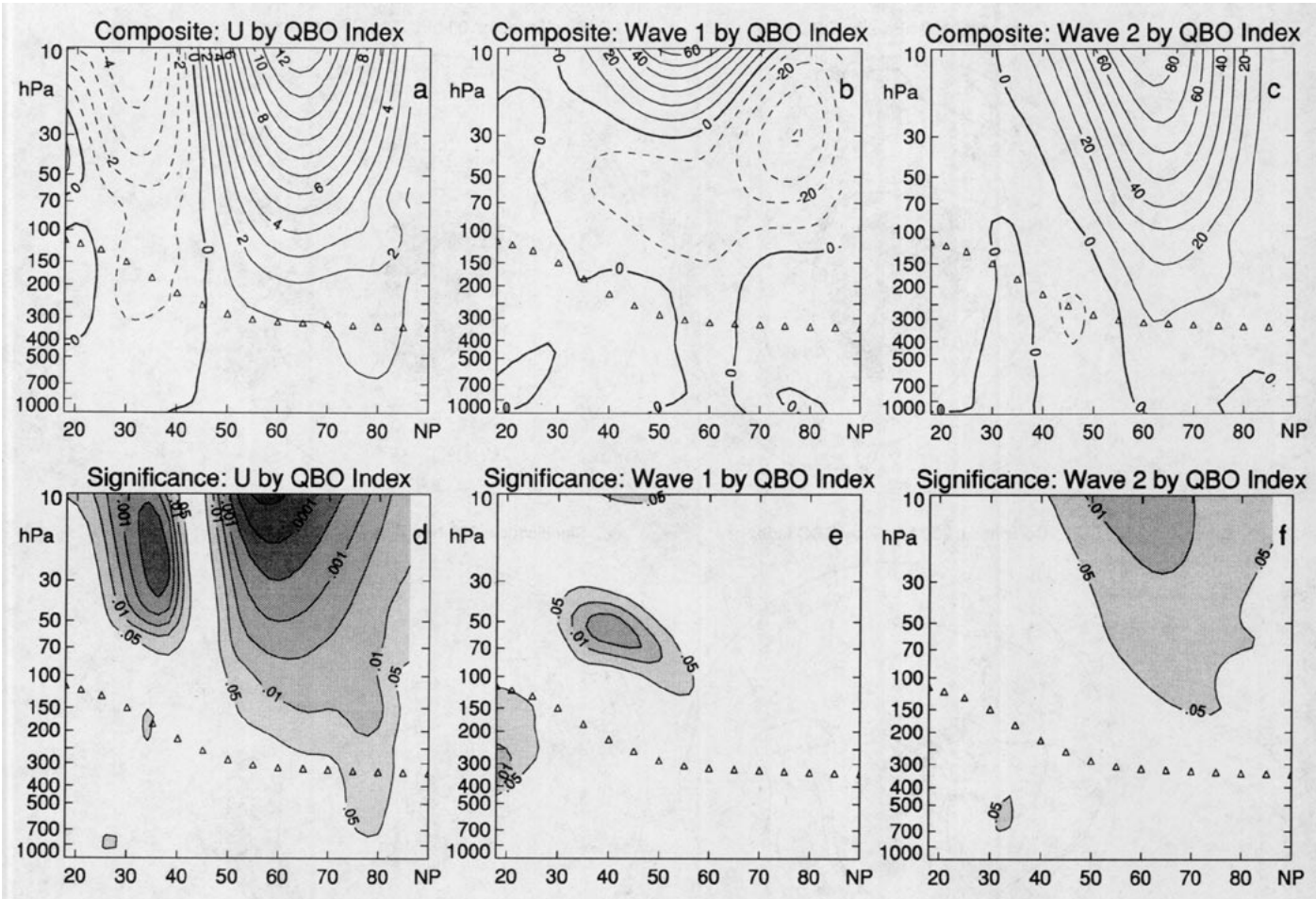

FIG. 11. As in Fig. 3 except the time series of the 40-hPa Singapore wind was used to create the composites.

gation of the polar 10-hPa pattern in Fig. 10, is locally significant over almost half the stratospheric grid.

It was shown in Dunkerton and Baldwin (1991) and Baldwin and Dunkerton (1991) that the Eliassen–Palm (EP) flux (Edmon et al. 1980) is modulated by the QBO. It is important to include the full transient wave field (daily data) in calculating the EP flux before performing the seasonal average, as it is primarily the transient rather than the stationary waves that are affected by the QBO. The EP flux (which represents the propagation of wave activity in the zonal-mean plane) and the divergence of this flux (which indicates forcing of the zonal flow by the waves) is modulated in a manner consistent with the difference in the zonal flow between the east and west phases of the QBO. Figure 12 illustrates the composite differences in the EP flux based on time series of the three tropospheric modes and the 40-hPa QBO.

The vectors do not represent absolute propagation but only a difference between composites of positive and negative values of the respective indices. Similarly, the EP flux divergence represents the difference between the two composites. Both the vectors and the divergence are scaled by a factor of $\cos^2\theta$. The EP flux divergence is somewhat noisy, so these EP flux calculations should be used only as an indication of the effect of the waves on the mean flow.

Only the QBO composite (Fig. 12d) shows a substantial response in the stratosphere. For the composites based on the tropospheric EOFs, the modulation of the EP flux divergence is confined mainly to the troposphere and the lowest parts of the low-latitude stratosphere. The upper tropospheric patterns of the difference in EP flux divergence for the three EOF-based composites are consistent with the respective modulation of zonal-mean wind (Figs. 3, 7, and 9). The modulation by the QBO is also seen in the middle stratosphere.[1]

[1] Baldwin and Dunkerton (1991), using data from 1978–1990 up to 1 hPa, showed (as their Fig. 5) a similar figure to Fig. 12d in which the response was much larger above 10 hPa. The modest features in Fig. 12d near 10 hPa appears to be the lowest extent of substantial EP flux divergence modulation by the QBO.

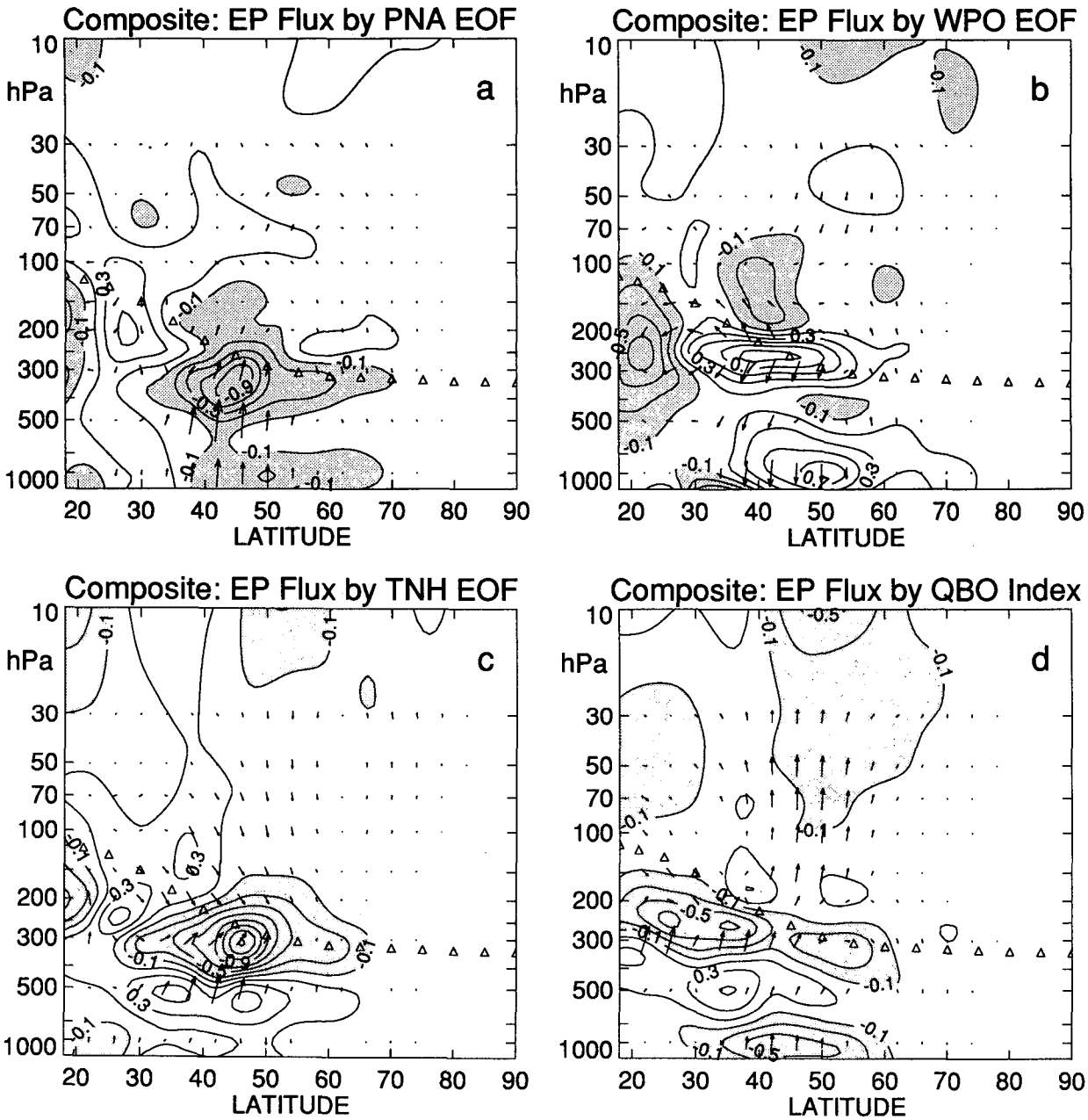

FIG. 12. Composite difference of Eliassen–Palm flux for all years when the time series of the expansion coefficients of the EOF was positive minus the average for all years when the time series was negative: (a) PNA-like mode, (b) WPO-like mode, and (c) TNH-like mode. The composite for panel (d) was created using the time series of the 40-hPa Singapore winds, using east minus west phase for comparison with Fig. 5 of Baldwin and Dunkerton (1991). Contours of the EP flux divergence are in m s^{-1} day^{-1}, multiplied by $\cos^2\theta$. The vectors have also been multiplied by $\cos^2\theta$. The triangles represent the approximate wintertime tropopause.

8. Discussion

ENSO has been linked to modulation of three modes of variability in the midlatitude troposphere: the PNA, WPO, and TNH patterns. These patterns may be characterized by three of the leading EOFs of the 500-hPa flow. If ENSO has a remote effect on the winter stratosphere, the signal may be communicated through the extratropical troposphere by modulation of these fundamental modes of variability.

Time series of the PNA, WPO, and TNH modes are represented by the amplitude of the principal component of rotated EOFs that correspond to the three patterns. The results of composites and correlations based on these time series of the PNA-, WPO-, and TNH-like modes show that the zonal-

mean wind responses to these patterns tend to decay in the lower stratosphere. The patterns in composite differences in geopotential appear to be genuine but fall below the 0.05 level of statistical field significance. With only 30 years of data, the statistical tests demand large amplitude composite differences over a substantial part of the hemisphere. If the composites truly are of only moderate strength, such tests will find that the patterns are not statistically significant. The stratospheric geopotential responses to all three modes project more onto zonal wave 2 than zonal wave 1. The wave-2 patterns associated with both the PNA- and WPO-like modes are field significant at the 0.05 level. The TNH wave-2 composite anomaly is slightly smaller but overall the TNH patterns had the lowest significance values, even in the troposphere.

Since alternative definitions of the amplitudes of the PNA, WPO, and TNH patterns might change these results, most of the composite differences were repeated using gridpoint-based time series of normalized geopotential anomalies (e.g., Wallace and Gutzler 1981). The results of these calculations did not differ substantially from those using EOF-based time series. The geopotential composites are very similar, with some differences in the amplitudes of wave 1 and wave 2. The PNA responses are nearly identical for EOF- and gridpoint-based time series. The WPO patterns using the gridpoint-based time series are slightly larger in both wave 1 and wave 2. The stratospheric TNH pattern based on the gridpoint index is dominated by wave 2 and is slightly weaker at 50 hPa than the EOF-based composite difference. The integrated t statistic for the gridpoint-based wave-2 TNH composite falls just below the 0.05 significance level.

A comparison with the stratospheric response associated with the QBO shows that the QBO's influence on the DJF-averaged circulation is primarily on the zonal-mean flow, whereas the association with the three tropospheric modes is mainly limited to wave components. In absolute terms, the QBO-based geopotential composites at 50 hPa are almost 300 m, compared with about 110 m for the PNA-like mode, 130 m for the WPO-like mode, and 150 m for the TNH-like mode. The QBO appears to be more important as a factor controlling the circulation of the polar stratosphere. The minimum temperatures reached in the polar vortex, of considerable importance in the formation of polar stratospheric clouds and attendant ozone depletion, require a strong, undisturbed polar vortex (Garcia and Solomon 1987). These are conditions primarily associated with the west phase of the QBO, but amplitudes of waves 1 and 2 could also influence conditions in the polar vortex (Baldwin and Holton 1988).

This paper examines only one possibility for a link between ENSO and the stratospheric flow. The focus of this paper is on linear relationships between time series of the amplitudes of three ENSO-related EOFs and the state of the stratosphere. The North Atlantic Oscillation (NAO) represents another tropospheric mode of variability. The NAO does appear to be linked to the state of the polar vortex (Baldwin et al. 1994). Other, nonlinear, relationships could be important. It is possible that a superposition of tropospheric modes may be associated with stratospheric variability or that there is a midlatitude response only during strong warm ENSO events. Perhaps the transmission of an ENSO signal through the midlatitude troposphere to the stratosphere could possibly be accomplished through mechanisms not considered in this paper.

Acknowledgments. This research has been supported by Grants ATM-9013280, ATM-933068, and ATM-945448 from the National Science Foundation and Grant NA90AA-D-AC807 from the National Oceanic and Atmospheric Administration. Partial computing support was provided by the University of Alaska Southeast. We wish to thank Dr. Robert Livezey and an anonymous reviewer for helpful comments on an earlier version of this paper, and Dr. Chidong Zhang for providing the Southern Oscillation index data.

REFERENCES

Angell, J. K., 1992: Evidence of a relation between El Nino and QBO, and for El Nino in 1991–1992. *Geophys. Res. Lett.*, **19**, 285–288.

Baldwin, M. P., and J. R. Holton, 1988: Climatology of the stratospheric polar vortex and planetary wavebreaking. *J. Atmos. Sci.*, **45**, 1127–1142.

——, and T. J. Dunkerton, 1991: Quasi-biennial oscillation above 10 mb. *Geophys. Res. Lett.*, **18**, 1205–1208.

——, X. Cheng, and T. J. Dunkerton, 1994: Observed correlations between winter-mean tropospheric and stratospheric circulation anomalies. *Geophys. Res. Lett.*, **21**, 2717–2720.

Barnston, A. G., and R. E. Livezey, 1987: Classification, seasonality and persistence of low-frequency atmospheric circulation patterns. *Mon. Wea. Rev.*, **115**, 1083–1126.

——, and ——, 1989: A closer look at the effect of the 11-year solar cycle and the QBO on Northern Hemisphere 700 mb height and extratropical North American surface temperature. *J. Climate*, **2**, 1295–1313.

Charney, J. G., and P. G. Drazin, 1961: Propagation of planetary-scale disturbances from the lower into the upper atmosphere. *J. Geophys. Res.*, **66**, 83–109.

Dunkerton, T. J., and M. P. Baldwin, 1991: Quasi-biennial modulation of planetary wave fluxes in the Northern Hemisphere winter. *J. Atmos. Sci.*, **48**, 1043–1061.

——, and ——, 1992: Modes of interannual variability in the stratosphere. *Geophys. Res. Lett.*, **19**, 49–52.

Edmon, H. J., B. J. Hoskins, and M. E. McIntyre, 1980: Eliassen–Palm cross sections for the troposphere. *J. Atmos. Sci.*, **37**, 2600–2616.

Fels, S. B., J. D. Mahlman, M. D. Schwarzkopf, and R. W. Sinclair, 1980: Stratospheric sensitivity to perturbations in ozone and carbon dioxide: Radiative and dynamical responses. *J. Atmos. Sci.*, **37**, 2265–2297.

Garcia, R. R., and S. Solomon, 1987: A possible relationship between interannual variability in Antarctic ozone and the quasi-biennial oscillation. *Geophys. Res. Lett.*, **14**, 848–851.

Geller, M. A., and M. Zhang, 1992: Sea surface temperatures, equatorial waves, and the quasi-biennial oscillation. Preprints, *Eighth*

Conf. on the Middle Atmosphere, Atlanta, GA, Amer. Meteor. Soc., 89–92.

Gray, W. M., J. D. Sheaffer, and J. Knaff, 1992: Hypothesized mechanism for the stratospheric QBO influence on ENSO variability. *Geophys. Res. Lett.,* **19,** 107–110.

Hamilton, K., 1993a: An examination of observed Southern Oscillation effects in the Northern Hemisphere stratosphere. *J. Atmos. Sci.,* **50,** 3468–3473.

——, 1993b: A general circulation model simulation of El Nino effects in the extratropical Northern Hemisphere stratosphere. *Geophys. Res. Lett.,* **20,** 1803–1806.

Hitchman, H. H., C. B. Leovy, J. C. Gille, and P. L. Bailey, 1987: Quasi-stationary zonally asymmetric circulations in the equatorial lower mesosphere. *J. Atmos. Sci.,* **44,** 2219–2236.

Holton, J. R., and H.-C. Tan, 1980: The influence of the equatorial quasi-biennial oscillation on the global circulation at 50 mb. *J. Atmos. Sci.,* **37,** 2200–2208.

——, and ——, 1982: The quasi-biennial oscillation in the Northern Hemisphere lower stratosphere. *J. Meteor. Soc. Japan,* **60,** 140–148.

Livezey, R. A., and W. Y. Chen, 1983: Statistical significance and its determination by Monte Carlo techniques. *Mon. Wea. Rev.,* **111,** 46–58.

——, and K. C. Mo, 1987: Tropical–extratropical teleconnections during the Northern Hemisphere winter. Part II: Relationships between monthly mean Northern Hemisphere circulation patterns and proxies for tropical convection. *Mon. Wea. Rev.,* **115,** 3115–3132.

Mo, K. C., and R. E. Livezey, 1986: Tropical–extratropical geopotential height teleconnections during the Northern Hemisphere winter. *Mon. Wea. Rev.,* **114,** 2488–2515.

Nigam, S., 1990: On the structure of the variability of the observed tropospheric and stratospheric-mean zonal wind. *J. Atmos. Sci.,* **47,** 1799–1813.

O'Sullivan, D. J., and R. E. Young, 1992: Modeling the quasi-biennial oscillation's effect on the winter stratospheric circulation. *J. Atmos. Sci.,* **49,** 2437–2448.

Richman, M. B., 1986: Rotation of principal components. *J. Climatol.,* **1,** 39–57.

Robinson, W. A., 1988: Analysis of LIMS data by potential vorticity inversion. *J. Atmos. Sci.,* **45,** 2319–2342.

van Loon, H., and K. Labitzke, 1987: The Southern Oscillation. Part V: The anomalies in the lower stratosphere of the Northern Hemisphere in winter and a comparison with the quasi-biennial oscillation. *Mon. Wea. Rev.,* **115,** 357–369.

Wallace, J. M., and D. S. Gutzler, 1981: Teleconnections in the geopotential height field during the Northern Hemisphere winter. *Mon. Wea. Rev.,* **109,** 784–812.

——, and F.-C. Chang, 1982: Interannual variability of the wintertime polar vortex in the Northern Hemisphere middle stratosphere. *J. Meteor. Soc. Japan,* **60,** 149–155.

Xu, J., 1992: On the relationship between the stratospheric quasi-biennial oscillation and the tropospheric Southern Oscillation. *J. Atmos. Sci.,* **49,** 725–734.

Yasunari, T., 1989: A possible link of the QBOs between the stratosphere, troposphere and sea surface temperature in the Tropics. *J. Meteor. Soc. Japan,* **67,** 483–493.